Deaging and Asymmetric Energy Landscapes in Electrically Biased Ferroelectrics

Goknur Tutuncu, Dragan Damjanovic, Jun Chen, and Jacob L. Jones

Phys. Rev. Lett. **108**, 177601 — Published 23 April 2012

DOI: 10.1103/PhysRevLett.108.177601

Deaging and asymmetric energy landscapes in electrically biased ferroelectrics

Goknur Tutuncu,[1] Dragan Damjanovic,[2] Jun Chen,[3] and Jacob L. Jones[1*]

[1]*Department of Materials Science and Engineering, University of Florida, Gainesville, FL 32611, USA*
[2]*Ceramics Laboratory, Institute of Materials, Swiss Federal Institute of Technology in Lausanne—EPFL, CH-1015 Lausanne, Switzerland*
[3]*Department of Physical Chemistry, University of Science and Technology Beijing, Beijing 100083, China*

In ferroic materials, the dielectric, piezoelectric, magnetic, and elastic coefficients are significantly affected by the motion of domain walls. This motion can be described as the propagation of a wall across various types and strengths of pinning centers that collectively constitute a force profile or energetic landscape. Biased domain structures and asymmetric energy landscapes can be created through application of high fields (such as during electrical poling), and the material behavior in such states is often highly asymmetric. In some cases, this behavior can be considered as the electric analogue to the Bauschinger effect. The present work uses time-resolved, high-energy X-ray Bragg scattering to probe this asymmetry and the associated deaging effect in the ferroelectric morphotropic phase boundary composition $0.36BiScO_3$-$0.64PbTiO_3$.

* Corresponding Author: email jjones@mse.ufl.edu, telephone 352-846-3788

Domain wall motion is known to significantly affect the dielectric, piezoelectric, and magnetic properties of ferroic materials [1-5]. The motion of a domain wall through the lattice can be described by a force profile which represents the distribution and strength of various pinning centers [6]. While the lattice itself contains periodic pinning centers (*i.e.*, the Peierls potential [7-10]), most ferroelastic domain wall widths span several unit cells and these intrinsic effects are typically negligible [11]. Much stronger pinning centers often exist in ferroelectrics including defect complexes, dislocations, and grain boundaries. The motion of domain walls across these strong pinning centers can be described as "jerks" [11]. Recent experimental [12] and theoretical [13] work has also highlighted that domain walls can interact strongly with neighboring domain walls, limiting or enhancing domain wall motion.

Some information about the energy landscape can be obtained from the measurement of macroscopic properties. For example, the field amplitude or frequency dependence of the electric-field-induced polarization [6, 14] and strain [4] can be used to assess the total influence of all extrinsic (nonlattice) effects including, *e.g.*, domain wall and interphase boundary motion. This is done by determining the relative nonlinear contributions in a property coefficient that is intrinsically only weakly nonlinear within certain field (E) ranges.

X-ray Bragg scattering is a versatile tool that can be used to investigate ferroelastic domain wall motion in polycrystalline materials. High-energy X-rays, for example, can penetrate a very large volume of material and scattering from different ferroelastic domain variants can be observed as a crystallographic texture [15]. The average displacement of domain walls can then be described by the changes in texture observed during some process such as electric field application. Because this approach measures the collective response of many local domain wall motion processes, it can be used to interpret the effect of domain wall motion on behavior measured at the macroscopic length scale. Moreover, time-resolved data acquisition techniques

in conjunction with such an experiment can help interpret property coefficients that are typically measured under alternating fields, *e.g.* piezoelectric and dielectric permittivity coefficients [16, 17]. Time-resolved, high-energy X-ray Bragg scattering is applied in the present work to measure the ferroelastic domain volume fractions under positive and negative polarity of the waveform separately. This information is then used to infer characteristics about the asymmetric energetic landscape in a poled ferroelectric. This approach is demonstrated on the morphotropic phase boundary (MPB) composition $0.36BiScO_3$-$0.64PbTiO_3$ [18] which simultaneously exhibits a high room temperature piezoelectric coefficient (d_{33} = 460 pC/N) and a high Curie temperature (T_c = 450°C) [19].

Samples were synthesized using solid state reaction of the oxides at 760°C for 5 hours. Sintering of pressed pellets was performed in a closed crucible at 1100°C for 1 hour while embedded in calcined powder of the same composition. The grain size is on the order of 1 μm. Laboratory X-ray diffraction confirmed phase purity and also indicated a mixture of polymorphs that is consistent with the compositional proximity to the MPB. Pellets were polished, silver electrodes were fired on the sample at 550°C for 30 min, and poled at 100°C for 10 min. Polarization in the poled state was measured using a ferroelectric analyzer (TF1000, aixACCT, Germany) and a sinusoidal waveform of frequency 0.1 Hz. X-ray diffraction from a synchrotron source was undertaken *in situ* during electric field application using high-energy X-rays at beamline 11-ID-C at the Advanced Photon Source (APS). An X-ray beam of energy 114 keV and size of 0.5 mm by 0.5 mm was incident upon a sample of approximate dimensions 1 mm × 1 mm × 5 mm. During the electric field application, diffraction patterns were measured in forward scattering geometry (transmission mode) on a Perkin Elmer amorphous silicon area detector placed approximately 1800 mm from the sample. Certain measurements employed stroboscopic

data acquisition, for which the electric field was synchronized with the detector electronics and a response of 50 different cycles was summed at particular time periods relative to the waveform. The angle between the electric field direction and the scattering vectors of planes being measured on the detector is $2\theta/2 \approx 1.5°$. In polycrystalline ferroelectric materials, planes at these angles to the field direction behave equivalently to those parallel to the field [16, 17].

The polarization of the poled samples in response to electric fields of varying amplitude is shown in Fig. 1(a). Hysteresis is apparent in the polarization behavior which indicates dominant domain wall motion contributions. Significant contributions of conductivity can be excluded using the analysis presented in Ref. [20]. The polarization behavior is notably asymmetric at certain electric field amplitudes. The maximum polarization values measured in the positive and negative field directions in Fig. 1(a) were used to calculate the positive and negative relative permittivity as a function of field amplitude and these values are shown in Fig. 1(b). The absolute values of relative permittivity and the linear field amplitude dependence are similar to those reported by Eitel *et al.* [21] and correspond to Rayleigh-like behavior. This behavior extends up to approximately 2 kV/mm, where the relative permittivity increases markedly due to the proximity to the ferroelectric coercive field.

The results in Figs. 1(a) and 1(b) demonstrate an asymmetric polarization response to a symmetric electric field. Asymmetric electric-field-induced polarization may be observed even in mono-domain single crystals, where the contribution of ferroelastic domain wall motion is not present [22]. Szigeti has even shown anharmonicity in the static dielectric constant of cubic alkali halide crystals [23]. In poled ferroelectric materials, this behavior can be associated with either an internal electric field developed during the poling process or result from an average polarization bias in the forward direction. Asymmetry may also be rationalized to occur from extrinsic effects where the extent of domain wall motion in the positive and negative directions

may differ [2, 24, 25]. Considering domain wall motion as the movement of domain walls across an energy landscape of pinning centers, such asymmetry in the degree of domain wall motion can be described using an asymmetric energy landscape about a mean domain wall position.

Figure 2(a) shows the X-ray diffraction pattern of crystallographic poles parallel to the electric field direction during the first application of a single bipolar waveform on an unpoled sample. The coercive fields ($\pm E_c$) of approximately ±2 kV/mm are indicated in Fig. 2(a) and correlate with strong changes in the intensity of the {002} diffraction peaks. These field amplitudes also correlate with the significant increase in relative permittivity shown in Fig. 1(b), confirming that the large increase in relative permittivity is the result of approaching the ferroelectric coercive field. After the measurements described in Fig. 2(a), the sample was exposed to a positive electric field of 3.6 kV/mm for 5 minutes to strengthen the domain alignment in the positive field direction through electrical poling. After poling, square wave electric fields of frequency 0.33 Hz and sequentially increasing amplitudes were applied and diffraction data were measured using the stroboscopic approach [16, 17]. Figure 2(c) shows representative {002} diffraction peaks measured for an electric field amplitude of 1.5 kV/mm [Fig. 2(d)]. The electrical poling and several lower electric field amplitudes were applied to the sample between the data measured in Figs. 2(a) and (c). Thus, the domain volume fractions and relative intensity ratios are not equivalent at similar field amplitudes in Figs. 2(a) and (c). In Fig. 2(c), the (002) and (200) peaks corresponding to the tetragonal phase in the sample show measurable changes in their respective intensities between positive and negative polarity; this measurement confirms 90° domain wall motion during subcoercive alternating electric fields.

The integrated intensities of the {002} peaks measured during both the positive and negative polarities of the electric field waveform were extracted by fitting the measured intensity profile to three Gaussian peaks; these three peaks represent the tetragonal (002) and (200) and the

pseudo-cubic (200) reflection of a second polymorph. The respective domain volume fractions of the tetragonal phase were calculated using the intensities of the tetragonal (200) and (002) peaks relative to the intensities measured in an initially unpoled sample [15]. The resulting parameter, η_{002}, describes the relative volume fraction of tetragonal 001-oriented crystallites (c-axis domains) in the direction parallel to the electric field in the poled sample relative to an unpoled sample (unpoled $\eta_{002} = 0$).

The domain volume fractions during the positive [$\eta_{002}(+)$] and negative [$\eta_{002}(-)$] polarity of the electric field waveform are shown in Fig. 3(a). The difference between these values, or the change in domain volume fraction ($\Delta\eta_{002}$) [16], is shown in Fig. 3(b). Within certain electric field regions, nearly linear trends in $\Delta\eta_{002}$ with electric field amplitude are shown in Fig. 3(b), correlating with the linear field-amplitude dependence of permittivity (Rayleigh behavior) in Fig. 1(b).

The behavior in Fig. 3(a) can be divided into three distinct regions. In the weak-field region (E<1 kV/mm), small differences are observed in the domain volume fractions measured between the positive and negative polarities of the waveform, which is further reinforced in Fig. 3(b) as a low $\Delta\eta_{002}$ value. Domain wall motion between the positive and negative polarity of the waveform is therefore minimal in this region. However, the weak-field region in Fig. 3(a) also demonstrates that the values of $\eta_{002}(+)$ and $\eta_{002}(-)$ decrease with increasing field amplitude. This can be attributed to a deaging effect, observed in other ferroelectric materials as an irreversible change (within the timeframe of the experiment) in property coefficients due to application of small alternating fields [26, 27]. In the present measurements, this effect is observed as a progressive change in the average domain volume fractions during application of small alternating fields. With increasing field amplitude in this weak-field region, the average η_{002} values decrease (towards the unpoled value of $\eta_{002} = 0$) without becoming completely depoled.

In the intermediate-field region (1 kV/mm < E < 2 kV/mm), the domain volume fractions in the positive and negative polarity behave differently with electric field amplitude. The value of $\eta_{002}(+)$ is mostly field-independent and the values remain below those measured initially at weak fields ($\eta_{002}\approx 0.4$). In contrast, $\eta_{002}(-)$ exhibits a stronger linear dependence on electric field amplitude than that observed in the weak-field region. These two behaviors of $\eta_{002}(+)$ and $\eta_{002}(-)$ collectively yield the linear field-dependence of $\Delta\eta_{002}$ shown in Fig. 3(b). A linear field-amplitude dependence of $\Delta\eta_{002}$ previously observed in other materials has been attributed to a Rayleigh-like behavior of domain walls across randomly distributed pinning centers [17]. The separation of $\eta_{002}(+)$ and $\eta_{002}(-)$ in the present work demonstrates the ability of this measurement to discriminate the respective domain orientation states during the positive and negative polarities of the electric field waveform. As a result, a linear dependence of $\Delta\eta_{002}$ on electric field amplitude can be dominantly attributed to the increased field-dependence of $\eta_{002}(-)$; that is, domain walls move more under negative than positive fields.

In the high-field region (E>2 kV/mm), $\eta_{002}(-)$ continues to decrease linearly while $\eta_{002}(+)$ increases. This results in a relatively larger slope of $\Delta\eta_{002}$ with field amplitude and defines the maximum upper limit of the Rayleigh region.

To further interpret the observed behaviors in different field amplitude regions, we use simplified schematics of energy landscapes in Fig. 4. These energy landscapes represent the collective response of domain walls to the applied field. The average energy landscape in a material with random potentials and without asymmetry is shown in Fig. 4(a); such a state may be found surrounding most domain walls prior to a biasing process such as electrical poling. Electrical poling involves the application of large positive electric fields for relatively long periods of time. Under such conditions, the fraction of 001-oriented domains parallel to the electric field increases at the expense of 100-oriented domains and domain walls become

positioned nearer strong pinning centers such as defect complexes, dislocations, and grain boundaries. In Fig. 4(b), a representative domain wall position after the electrical poling process is shown as position (i). In the weak-field region (E<1 kV/mm), the perturbation of domain walls locally by small alternating electric fields can result in a progressive reverse motion of the domain walls towards a position of lower global energy [position (ii)]. This deaging effect can be described as a decrease in the median position of the domain volume fractions (η_d) with increased electric field cycling using an equation of the form,

$$\eta_d = \eta_{002,i} - m \cdot E, \quad (1)$$

where $\eta_{002,i}$ is the initial domain volume fraction and m is the deaging coefficient. The deaging coefficient, m = 0.021 mm/kV in the present work, is expected to be a function of the material and poling state as well as the loading conditions (*e.g.*, the waveform type, field amplitude steps, number of cycles measured at each field amplitude, etc.)

In the intermediate-field region (1 kV/mm < E < 2 kV/mm), we consider the behavior of a domain wall at the de-aged position (ii) in Fig. 4(b). The motion in the positive field direction is constrained by large pinning centers at fixed locations, constraining the values of $\eta_{002}(+)$ to those of the originally poled state [$\eta_{002}(+) < 0.4$, Fig. 3(a)]. If one considers motion in the negative field direction from position (ii) as small Barkhausen jumps or "jerks" [11] across randomly distributed pinning centers, a Rayleigh-like behavior would be expected. The linear field-amplitude dependence of $\eta_{002}(-)$ in the intermediate-field region confirms this type of irreversible domain wall displacement and the nature of the collective energy landscape in the reverse direction relative to forward (poling) direction.

The deaging effect may be assumed to extend into the intermediate (1 kV/mm < E < 2 kV/mm) and high-field (E > 2 kV/mm) regions as shown in Fig. 3(a). In this case, the deviation of $\eta_{002}(+)$ and $\eta_{002}(-)$ from η_d, or the deviation of domain volume fractions during positive and

negative polarity from the extrapolated de-aged position, is symmetrical as shown in Fig. 3(c). In this way, the deaging coefficient calculated from the weak-field region can be shown to characterize the asymmetry of the energy landscape.

Biased ferroelectric domain structures created through application of stress or electric fields have been considered as electric analogues to the Bauschinger effect observed in plastically deformed metals [28-30]. The Bauschinger effect, wherein the yield stress in the reverse direction (relative to initial deformation) is lower than that in the forward direction, can be described using an asymmetric energy landscape for dislocation motion; motion in the reverse direction is favored over the forward direction at a particular stress amplitude. In metals, the origin of this effect is related to either the dissolution of dislocation walls upon stress reversal or the relief of intergranular stresses [31]. The present use of Bragg diffraction enables the measurement of the analogous effect in ferroelectrics and, notably, the effect of the asymmetric energy landscape created through the electrical poling process on the deaging present during subsequent electric field cycling. Bragg diffraction is particularly suited for observing such phenomena because it can exclusively measure the collective motion of domain walls. The origin of the asymmetry in the present work has been described by the rearrangement of domain walls relative to pinning centers.

In summary, X-ray Bragg diffraction has been used in time-resolved, stroboscopic mode to measure the domain volume fractions in a ferroelectric during the positive and negative polarities of a symmetric bipolar waveform. A deaging effect consisting of an average movement of domain walls backwards, closer to the unpoled state, was observed during weak field cycling and described using an energy landscape associated with domain walls and pinning centers. The difference in domain volume fractions between the positive and negative polarities was also

found to be field-dependent, correlating with the Rayleigh behavior of permittivity in the same field-amplitude region.

JJ and GT acknowledge support from the U.S. Department of the Army under W911NF-09-1-0435, JC from the National Natural Science Foundation of China (Grants 91022016 and 21031005), and DD from the Swiss National Science Foundation. Use of the APS was supported by the U.S. Department of Energy, Office of Science, Office of Basic Energy Sciences, under Contract No. DE-AC02-06CH11357. The authors gratefully acknowledge Yang Ren and Guy Jennings for assistance with the diffraction measurements.

References

[1] X. L. Zhang *et al.*, Journal of Materials Science **18**, 968 (1983).
[2] S. P. Li, W. W. Cao, and L. E. Cross, J. Appl. Phys. **69**, 7219 (1991).
[3] Q. M. Zhang *et al.*, J. Appl. Phys. **75**, 454 (1994).
[4] D. Damjanovic, and M. Demartin, Journal of Physics-Condensed Matter **9**, 4943 (1997).
[5] L. Dante *et al.*, Phys. Rev. B **65**, 144441 (2002).
[6] O. Boser, J. Appl. Phys. **62**, 1344 (1987).
[7] R. E. Peierls, *Quantum Theory of Solids* (Oxford University Press, London, 1955).
[8] R. Landauer, J. Appl. Phys. **28**, 227 (1957).
[9] K. S. Novoselov *et al.*, Nature **426**, 812 (2003).
[10] H. Z. Ma *et al.*, Phys. Rev. Lett. **91**, 217601 (2003).
[11] R. J. Harrison, and E. K. H. Salje, Appl. Phys. Lett. **99**, 151915 (2011).
[12] P. Bintachitt *et al.*, P. Natl. Acad. Sci. USA **107**, 7219 (2010).
[13] E. K. H. Salje *et al.*, Phys. Rev. B **83**, 104109 (2011).
[14] D. A. Hall, Journal of Materials Science **36**, 4575 (2001).
[15] J. L. Jones, E. B. Slamovich, and K. J. Bowman, J. Appl. Phys. **97**, 034113 (2005).
[16] J. L. Jones *et al.*, Appl. Phys. Lett. **89**, 092901 (2006).
[17] A. Pramanick *et al.*, J. Am. Ceram. Soc. **94**, 293 (2011).
[18] R. E. Eitel *et al.*, J. Appl. Phys. **96**, 2828 (2004).
[19] R. E. Eitel *et al.*, Japanese Journal of Applied Physics Part 1-Regular Papers Short Notes & Review Papers **41**, 2099 (2002).
[20] D. Damjanovic, in *The Science of Hysteresis*, edited by I. Mayergoyz, and G. Bertotti (Elsevier, 2005), pp. 337.
[21] R. E. Eitel, T. R. Shrout, and C. A. Randall, J. Appl. Phys. **99**, 124110 (2006).
[22] R. A. Cowley, Reports on Progress in Physics **31**, 123 (1968).
[23] B. Szigeti, Proceedings of the Royal Society of London Series A-Mathematical and Physical Sciences **261**, 274 (1961).
[24] D. A. Hall, and M. M. Ben-Omran, Journal of Physics-Condensed Matter **10**, 9129 (1998).
[25] D. A. Hall, M. M. Ben-Omran, and P. J. Stevenson, Journal of Physics-Condensed Matter **10**, 461 (1998).
[26] V. Mueller, and Q. M. Zhang, Appl. Phys. Lett. **72**, 2692 (1998).
[27] D. V. Taylor, and D. Damjanovic, Appl. Phys. Lett. **73**, 2045 (1998).
[28] J. E. Huber, *Ferroelectrics: Models and Applications* (University of Cambridge, 1998), p. 172.
[29] J. E. Huber *et al.*, Journal of the Mechanics and Physics of Solids **47**, 1663 (1999).
[30] C. M. Landis, and R. M. McMeeking, Proceedings of the SPIE **3667**, 172 (1999).
[31] S. Suresh, *Fatigue of Materials* (Cambridge University Press, 1998), p. 679.

Figure Captions

Figure 1. (a) Polarization of BS-64PT to varying electric field amplitudes. (b) Relative permittivity measured in the positive and negative field directions as a function of electric field amplitude.

Figure 2. (a) Diffraction intensities of {002} reflections parallel to the electric field amplitude during application of a bipolar triangular wave, (b). (c) Diffraction intensities of {002} reflections parallel to the electric field amplitude during application of a square bipolar electric field of 1.5 kV/mm and frequency 0.33 Hz, (d).

Figure 3. (a) Fraction of 001-oriented domains parallel to the electric field during the application of positive and negative electric field amplitudes [$\eta_{002}(+)$ and $\eta_{002}(-)$]. All values calculated from {002} diffraction intensities. (b) The change in domain fractions between the positive and negative states ($\Delta\eta_{002}$). (c) The deviation of $\eta_{002}(+)$ and $\eta_{002}(-)$ from the deaging equation (η_d).

Figure 4. Schematics of energy functions U(s) for domain wall displacements, s. (a) Position of a domain wall random potentials and without asymmetry. (b) Position of a domain wall after strong electric field applied towards the right hand side (positive) in (i); de-aged position of a domain wall in (ii).

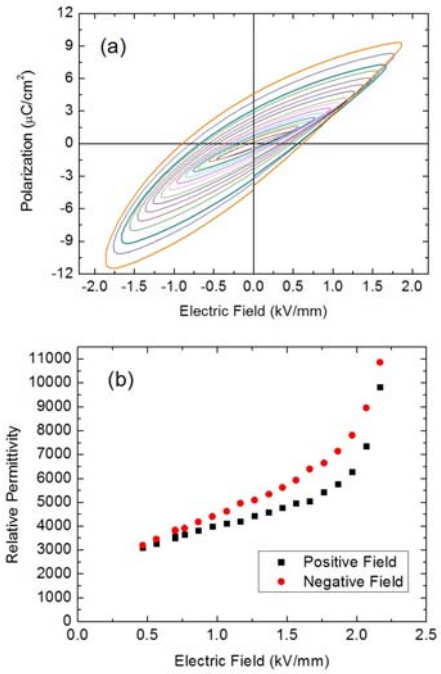
(a)
Polarization (μC/cm²)
Electric Field (kV/mm)
(b)
Relative Permittivity
Positive Field
Negative Field
Electric Field (kV/mm)

Figure 1.

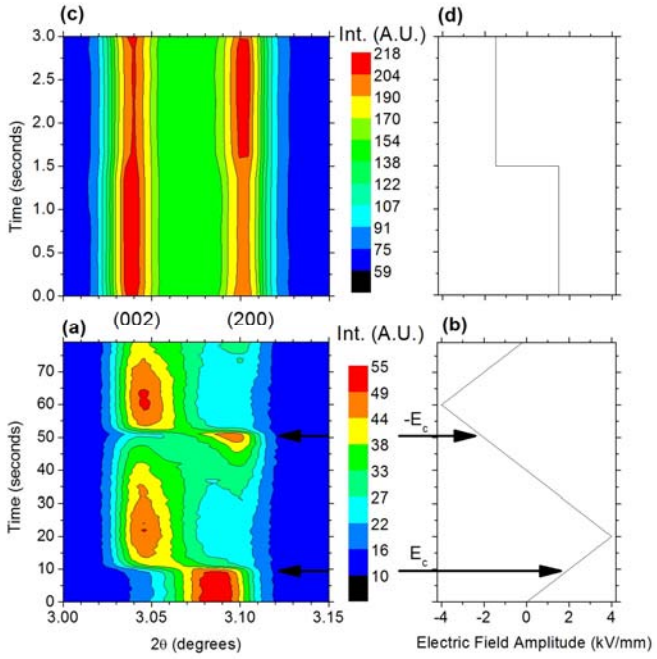
(c)
(d)
Int. (A.U.)
218
204
190
170
154
138
122
107
91
75
59
Time (seconds)
3.0
2.5
2.0
1.5
1.0
0.5
0.0
(a)
(002)
(200)
Int. (A.U.)
(b)
55
49
44
38
33
27
22
16
10
-E_c
E_c
70
60
50
40
30
20
10
0
3.00
3.05
3.10
3.15
2θ (degrees)
-4
-2
0
2
4
Electric Field Amplitude (kV/mm)

Figure 2.

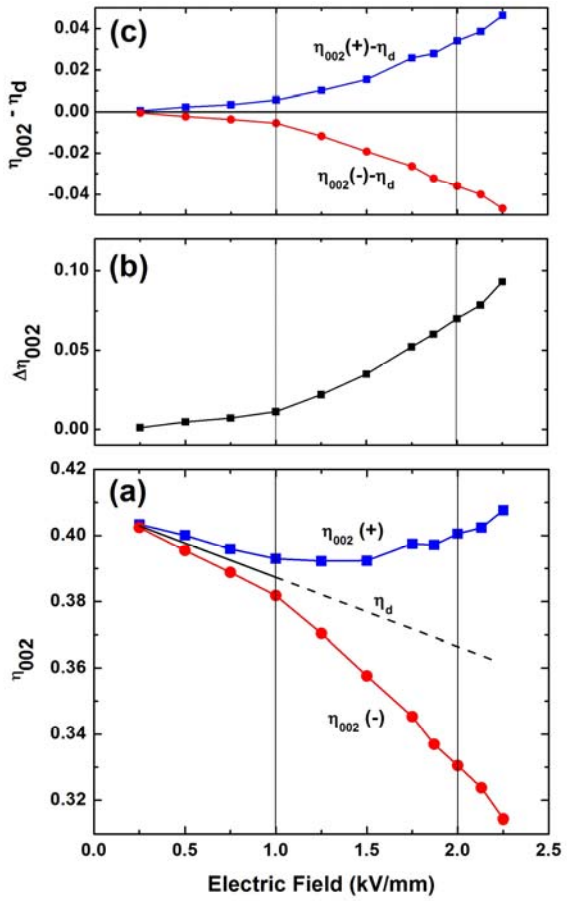
(c)
$\eta_{002}(+)-\eta_d$
$\eta_{002}(-)-\eta_d$
$\eta_{002} - \eta_d$
0.04
0.02
0.00
-0.02
-0.04
(b)
$\Delta\eta_{002}$
0.10
0.05
0.00
(a)
η_{002} (+)
η_d
η_{002} (-)
η_{002}
0.42
0.40
0.38
0.36
0.34
0.32
0.0
0.5
1.0
1.5
2.0
2.5
Electric Field (kV/mm)

Figure 3.

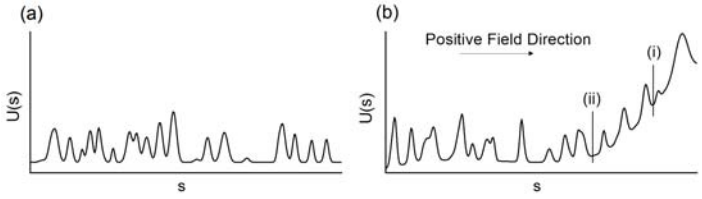

Figure 4.